$Na_3V_2(PO_4)_3$ - a highly promising anode and cathode material for sodium-ion batteries

*Tolga Akçay [a], Marcel Häringer [a], Kristina Pfeifer [a], Jens Anhalt [a], Joachim R. Binder [a], Sonia Dsoke [a,b], Dominik Kramer *[a], and Reiner Mönig [a]*

[a] Institute for Applied Materials (IAM), Karlsruhe Institute of Technology (KIT), Hermann-von-Helmholtz-Platz 1, 76344 Eggenstein-Leopoldshafen, Germany

[b] Helmholtz-Institute Ulm for Electrochemical Energy Storage (HIU), P.O. Box 3640, 76021 Karlsruhe, Germany

Keywords: $Na_3V_2(PO_4)_3$; NASICON; cathodes; anodes; full cells; symmetric cells; degradation; sodium-ion batteries.

Abstract

Sodium-ion batteries may develop into a cost-efficient alternative to lithium-ion batteries. $Na_3V_2(PO_4)_3$/C (NVP/C) is known to be a suitable electrode material for such batteries that can be used as anode or cathode. Here, NVP/C-based electrodes were investigated in different cell configurations. The electrodes were cycled against the anode materials hard carbon, Sb/C, SnSb/C and sodium metal. Furthermore, NVP versus NVP was investigated. When NVP/C is cycled against the other anode materials, the cells exhibit relatively poor reliability, but in NVP-NVP cells a high cycling stability was observed and more than 1500 cycles with a capacity retention of 80 % were achieved. This work demonstrates that common problems of Na and Na-ion cells result from the anode materials used and that NVP/C itself is very reliable both as anode and cathode material.

1.) Introduction

Low-cost electrochemical energy storage has been considered as a key factor to enable a smart grid that uses a larger fraction of renewable energies [1]. High-temperature sodium-based batteries, mainly sodium-sulfur systems, have already been installed for large-scale energy storage [2]. Recently, considerable research efforts have been made aiming at room temperature sodium-ion secondary batteries (SIB). Although significant progress has been achieved, long-term stability over many charge-discharge cycles – which directly determines the total cost of ownership of the battery – is still challenging. An electrode material that is promising with respect to high stability over many cycles is sodium vanadium phosphate $Na_3V_2(PO_4)_3$ (NVP). It features a highly stable three-dimensional network of a NASICON (NA Super Ionic CONductor) structure and offers large Na diffusion pathways [3, 4, 5]. Owing to its poor electronic conductivity, the particle size should be small; alternatively, a carbon coating can be applied to obtain NVP/C composites

with acceptable rate capability [6, 7, 8]. The as-synthesized NVP can accept or release sodium ions and therefore it can be used as negative or positive electrode material [9, 10, 11]. Two different voltage plateaus are associated with two-phase transitions: the transition at 3.4 V vs. Na/Na^+ matches the application of a cathode material, whereas the transition at 1.7 V vs. Na/Na^+ can be used for an anode material. The resulting redox couple V^{4+}/V^{3+} from the reaction of $Na_3V_2(PO_4)_3$ to $NaV_2(PO_4)_3$ at 3.4 V provides a theoretical capacity of 117.6 mAh/g and involves the deinsertion/insertion of two sodium ions. In contrast, the insertion/deinsertion of a single ion is suggested for the electrochemical reaction at 1.7 V. Consequently, the reversible capacity is only 58.8 mAh/g in the potential region between 3 V and 1 V vs. Na/Na^+ [9, 11]. Besides these reasonable capacity values, the material is also expected to exhibit good rate capability and high stability due to its NASICON-type structure. In the literature, most of these key properties have been experimentally confirmed [12]; however, in many cases, the reported cycling stability was limited [2, 13, 14, 15, 16]. An extremely high cycling stability was reported for an NVP-NVP cell with an ether-based electrolyte [17]. Furthermore, NVP-NVP cells have been investigated for all-solid-state SIB [18, 19]. In this work, we aim to clarify the discrepancies in the reliability of NVP and investigate the origins of degradation by comparing the performance of NVP in various electrolytes and different configurations. The results show that, when combined with a stable counter electrode, NVP is very reliable: It achieves more than 1500 cycles with a capacity retention of 80 % and a specific current of 100 mA/g.

2.) Materials and methods

2.1) Electrode materials

The NVP/C composites were synthesized via spray-drying with a subsequent calcination. For this, ammonium metavanadate (NH_4VO_3, Honeywell), sodium carbonate (VWR) and ammonium

dihydrogen phosphate (VWR) were dispersed in absolute ethanol (VWR) in a molar ratio of 4:3:6. Polyacrylic acid (Sigma Aldrich) and β-lactose (Sigma Aldrich) were optionally subjoined in 16.7 wt%. The reactants were milled in a planetary ball mill for 5 h. The suspension was spray-dried with an inlet-temperature of 150 °C and an outlet-temperature of 95 °C. The precursor was heated with a heating rate of 5 K/min to 400 °C and held for 4 h. Subsequently, the temperature was increased with the same rate to 850 °C followed by a dwell time of 12 h. After cooling down, the NVP/C composite was mixed with polyvinylidene fluoride (PVDF, Sigma Aldrich) and the conductive carbon additive TIMCAL-C65 in a weight ratio of 80:10:10. NMP was added as solvent and the obtained paste was coated onto aluminium foil, using a doctor blade with a gap size of 200 µm. The cast films were dried in two steps, first for 30 minutes at 80 °C in air and at 120 °C under vacuum for 12 h. The active material loading per unit area amounts to 3.34 mg/cm².

For the anodes, 85 % hard carbon (HCC, Xiamen Tmax Battery Equipments), 5 % C65 conductive agent, and 10 % CMC as binder were used, unless otherwise specified. As raw material for tin and antimony-based anodes, tin nanopowder (Sigma Aldrich, USA, ≥99 % trace metals basis) and antimony powder (Alfa Aesar, USA, 200 mesh, 99.999 % metals basis) were used. SnSb was synthesized by mixing a 1:1 molar ratio of Sn and Sb and subsequent reactive milling for 30 h. These raw materials were mixed with 30 wt% of C65 as conductive carbon and milled for 15 h to obtain the active material, with breaks after every 15 min of milling to reduce the temperature in the ball mill.

2.2) Electrolyte preparation and cell assembly

For the standard electrolyte in cell configurations against sodium metal, vacuum dried $NaClO_4$ (1 mol/l) was dissolved in an EC/DMC 1:1 mixture with 5 wt% of FEC. In the sodium metal cells,

Na metal discs with a diameter of 12 mm were used and excess Na was available due to the thickness of the discs. Two-electrode setups were obtained by assembling Swagelok-type cells in an Ar-filled glovebox, whereas custom built PEEK (polyether ether ketone) cells were used for three-electrode measurements according to literature [20, 21]. The latter setup consists of a working and a counter electrode positioned between spring-loaded titanium pistons. The sodium reference electrode is placed on a compressed glass fiber separator (Whatman GF/D) in a cavity close to the working electrode/counter electrode stack and is contacted by a titanium screw. In both types of cell setups, glass fiber separators (Whatman GF/B or GF/D) with a diameter of 12 mm were used. All cell parts and electrodes were dried at 120 °C. Each cell was filled with 0.1 ml of electrolyte.

2.3) Electrochemical experiments

In this work, the specific currents and capacities are calculated regarding the active mass of the NVP/C cathode, whereas for full cells with HCC, Sb/C and SnSb/C the total active mass of the anode and cathode is considered. An electrochemical galvanostat/potentiostat (Bio-Logic, VMP3) was used for the galvanostatic cycling with potential limitation (GCPL) and for the cyclic voltammetry (CV). Concerning the GCPL measurements, the majority of our cells were operated at room temperature in a two-electrode configuration in the voltage range between 2.3 V and 3.9 V vs. Na/Na^+ with a specific current of 100 mA/g. For the CV measurements, a three-electrode configuration in the voltage range between 1.45 V and 1.85 V vs. Na/Na^+ or between 3.2 V and 3.6 V vs. Na/Na^+ with a scan rate of 0.025 mV/s was used in a climate chamber at 25 °C.

3.) Results and discussion

3.1) Electrochemistry of NVP/C

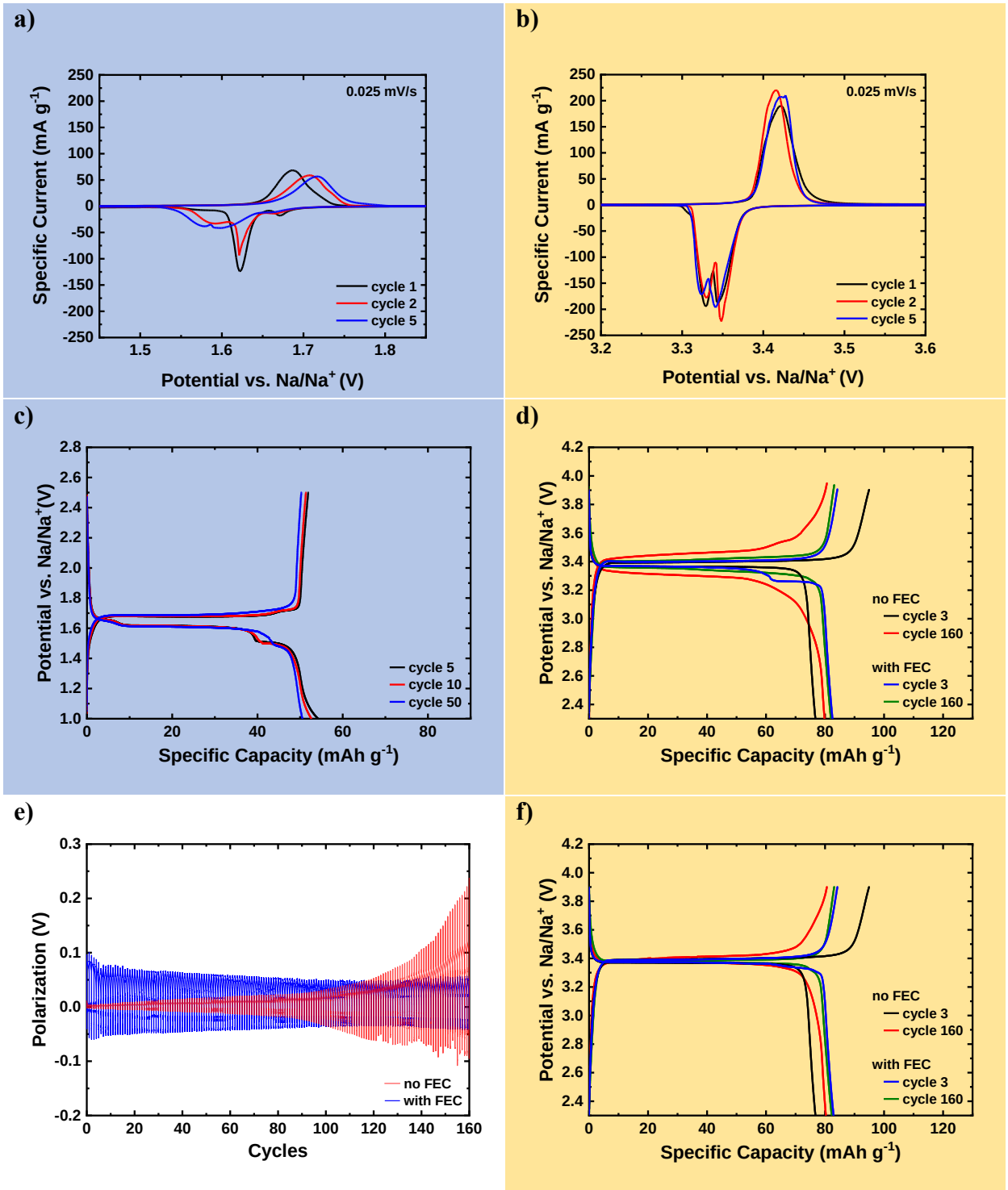

Figure 1. Electrochemical data of NVP/C cycled against sodium metal with 1 M $NaClO_4$ in EC/DMC (1:1) + 5 wt% FEC (a-f) and without FEC (d-f). Data from the lower voltage region (anode material range) is plotted on a blue background and data from the higher voltage region (cathode material range) is plotted on a yellow background. (a) CV of NVP/C in the voltage range between 1.45 V – 1.85 V vs. Na/Na^+ and (b) 3.2 V – 3.6 V vs. Na/Na^+; (c) GCPL curves of NVP/C (1 V – 2.5 V vs. Na/Na^+) in a two-electrode configuration with a specific current of 18 mA/g; (d) GCPL curves of NVP/C (2.3 V – 3.9 V vs. Na/Na^+) evaluated as a two-electrode configuration with a specific current of 18 mA/g; (e) polarization (potential of Na counter electrode vs. Na reference electrode) over cycles without FEC (red) or with 5 wt% FEC (blue) and (f) GCPL curves of NVP/C (2.3 V – 3.9 V vs. Na/Na^+) in a three-electrode configuration with a specific current of 18 mA/g.

As a first step, the electrochemical behaviour of NVP/C against sodium was characterized to better understand the properties of the NVP/C electrode. Therefore, CVs were measured in two voltage ranges: 1.45 V to 1.85 V and 3.2 V to 3.6 V vs. Na/Na^+ with a scan rate of 0.025 mV/s. During the first cycle, a peak pair during reduction is observed between 1.62 V and 1.67 V (Fig. 1a) and a single peak during oxidation is observed at 1.69 V; these are the redox processes of the V^{3+}/V^{2+} redox couple where the as-prepared NVP/C accepts Na^+ and could therefore be used as anode material (Fig. 1a). Fig. 1b shows a single peak during oxidation in the first cycle at 3.42 V and a peak pair during reduction between 3.32 V and 3.35 V; these are the redox processes of the V^{4+}/V^{3+} redox couple where two Na^+ can be extracted from the as-prepared NVP/C and therefore NVP/C can be used as cathode material. The peaks during reduction (Fig. 1a) broaden significantly during the first few cycles. The specific charge of the NVP/C, which is obtained by the integration of the CV curves (Fig. 1a, b), is twice the amount for the V^{4+}/V^{3+} redox couple compared to the V^{3+}/V^{2+}

redox couple. This is in line with the amount of sodium ions that can be inserted/extracted into/from the active material.

Most studies report single peaks during oxidation between 3.4 V and 3.54 V and during reduction between 3.15 V and 3.3 V, corresponding to the V^{4+}/V^{3+} redox reactions ($Na_3V_2(PO_4)_3$ / $NaV_2(PO_4)_3$), as well as electrochemical activity at 1.63 V during reduction due to the redox couple V^{3+}/V^{2+} [11, 22, 23, 24]. Jiang et al. [25] report that the two reduction peaks at 3.2 V and 3.33 V for V^{4+}/V^{3+} appear in the first cycles and slowly fade into one in the following cycles. They associate the second peak at lower potential with a transfer from Na1 to Na2 ion sites, causing a rearrangement in the local redox environment.

NVP/C demonstrates good cycling stability when cycled at 18 mA/g (ca. 0.15 C) up until 1180 mA/g (ca. 10 C) between 2.3 V and 3.9 V in a two-electrode configuration versus Na/Na^+. NVP/C was also cycled at lower voltages between 1 V and 3 V. It exhibits a clear-cut plateau around 1.6 V (Fig. 1c), which is advantageous for the use as anode material in batteries. In Fig. 1d and 1f, representative charge/discharge curves of different cycles are presented. The long plateau around 3.4 V (Fig. 1d) is stable for more than 160 cycles and matches the results from the CV measurement (Fig. 1b).

Fig. 1d and 1f contain the same data plotted in different ways. Fig. 1d shows the potential curve of the working electrode (WE) measured against the counter electrode, while Fig. 1f displays the potential of the working electrode against the reference electrode (RE). If the voltage is measured against RE, a single plateau is observed in the GCPL measurements (Fig. 1f). A second voltage plateau at the end of the sodiation step, as visible in the blue curve of Fig. 1d, can only be observed when the WE is measured against the counter electrode. This clearly indicates that the voltage drop originates from the counter electrode.

Such a second plateau shifted by roughly 0.1 V has already been reported in previous works on NVP/C [6, 26, 27, 28, 29, 30]. Depending on the authors, effects either on the anode or on the cathode side are held responsible: On the one hand, Jiang et al. [28] attributed the second plateau to reactions on the sodium metal surface. On the other hand, later publications attributed this effect to the cathode material [27, 30]. Chen et al. [27] correlated the lower voltage plateau to the previously mentioned two reduction peaks in the CV measurements (Fig. 1b). This was ascribed to a two-step Na diffusion process caused by slow intercalation kinetics at high rates [29, 30]. Hence, the real origin of this phenomenon is not fully clear yet. These double peaks appear in the CV of Fig. 1b, where the potential was measured against the reference of the three-electrode configuration. This shows that they originate from processes in the cathode. The two reduction peaks in the CV and the second plateau caused by the voltage drop are two independent events. This can be seen in Fig. S1a, where the appearance of the second plateau coincides with an increasing polarization of the anode. This phenomenon only occurs when sodium metal anodes are used in an electrolyte with FEC. The shape of the plateau can vary, as seen in Fig. 3a/b and in literature, similar plateaus can be found in cells without NVP [31, 32]. Therefore, at high voltage NVP/C exhibits only one long plateau and is a promising cathode material for cells with relatively high energy density. Its performance with different anode materials will be addressed in the following paragraphs.

3.2) NVP/C cycled against HCC, Sb/C, and SnSb/C

Here, we investigate the behaviour of NVP/C in full cells with 1 M $NaClO_4$ in EC/DMC (1:1) (5 wt% FEC) containing HCC, Sb/C and SnSb/C anodes. For NVP-SnSb cells, an anode/cathode mass ratio of 0.19 in a voltage window between 1.8 V and 3.6 V was used. Likewise, NVP-Sb was cycled between 1.8 V and 3.6 V with a ratio of 0.14 and NVP-HCC between 1.5 V and 3.6 V with

a ratio of 0.22. In all three cell configurations (Fig. 2a), the initial full cell discharge capacity ranges between 43 and 46 mAh/g per total active mass and the capacity fades rapidly in the following cycles. The initial Coulombic efficiency (CE) for all three cells is between 62 % and 66 %. The NVP-HCC full cell exhibits higher CE in the subsequent cycles, reaching 98 %, while the cells with conversion anodes reach a maximum of 96 %. Since the NVP/C reaches a CE over 99.5 % when cycled versus sodium metal, the lower values in full cells indicate that the CE is mostly limited by the anode material. The lower CE of alloy-based anodes compared to the HCC might be influenced by the phase transformations and the associated large volume changes. Since the experiments have been performed in three-electrode cells, the potentials of the anode, cathode, and the voltage of the full cell are plotted in Fig. 2b-d. During charge, the potential of the NVP/C exceeds the potential of the plateau demonstrating that all of its sodium can be extracted. During discharge, the potential of NVP/C does not fall below the plateau at 3.35 V (Fig. 1f) even though the initial potential of the uncycled cathode is between 2.8 V and 2.9 V vs. Na/Na^+ (Fig. 2b). This behaviour is independent of the used anode material (Fig. 2b-d). It shows that the amount of sodium inserted into NVP/C is lower than the one that was extracted, indicating that the sodium is captured at the anode side due to irreversible processes.

This leads to a shortening of the NVP/C plateau during cycling. The potentials at maximum sodiation of both anodes containing Sb (Fig. 2c,d) shift upwards upon cycling due to incomplete sodiation and therefore a misbalancing. This causes a rise in the potentials of the NVP/C when fully desodiated. Besides the truncation around the point of maximum sodiation, the overall shape of the anode potential profile remains similar, but becomes contracted along the horizontal axis upon cycling. This may be explained by the loss of active material. Such an effect is not present in NVP-HCC full cells, where, besides the first sodiation, the slope of the anode potential does not

significantly change during the first ten cycles (Fig. 2b). Nevertheless, the shifts indicate a strong loss of cyclable sodium in the cell. Since in an NVP-Na metal cell 160 cycles were achieved (Fig. 1d, f), possible explanations for the loss of sodium include the options of Na trapping in the negative electrode or in a growing solid electrolyte interphase (SEI) [33]. Comparing the full cells assembled, the hard carbon-based one shows the best capacity retention and the Sb-based cells exhibit a voltage plateau around 0.5 V, which results in a smaller variation of cell voltage (Fig. 2). Based on our findings for NVP/C, it may be concluded that the investigations of cathode materials are facing major challenges in sodium metal counter electrode setups, which will be discussed in the following section. This is in line with the thus far reported literature [21, 34]. Additionally, our study reveals that in full cell setups with common anode materials, these materials suffer from irreversible losses. The anode materials constantly consume sodium and without presodiation of the anode materials or even an artificial SEI prior to the cell assembly, the lifetime of the cells is limited.

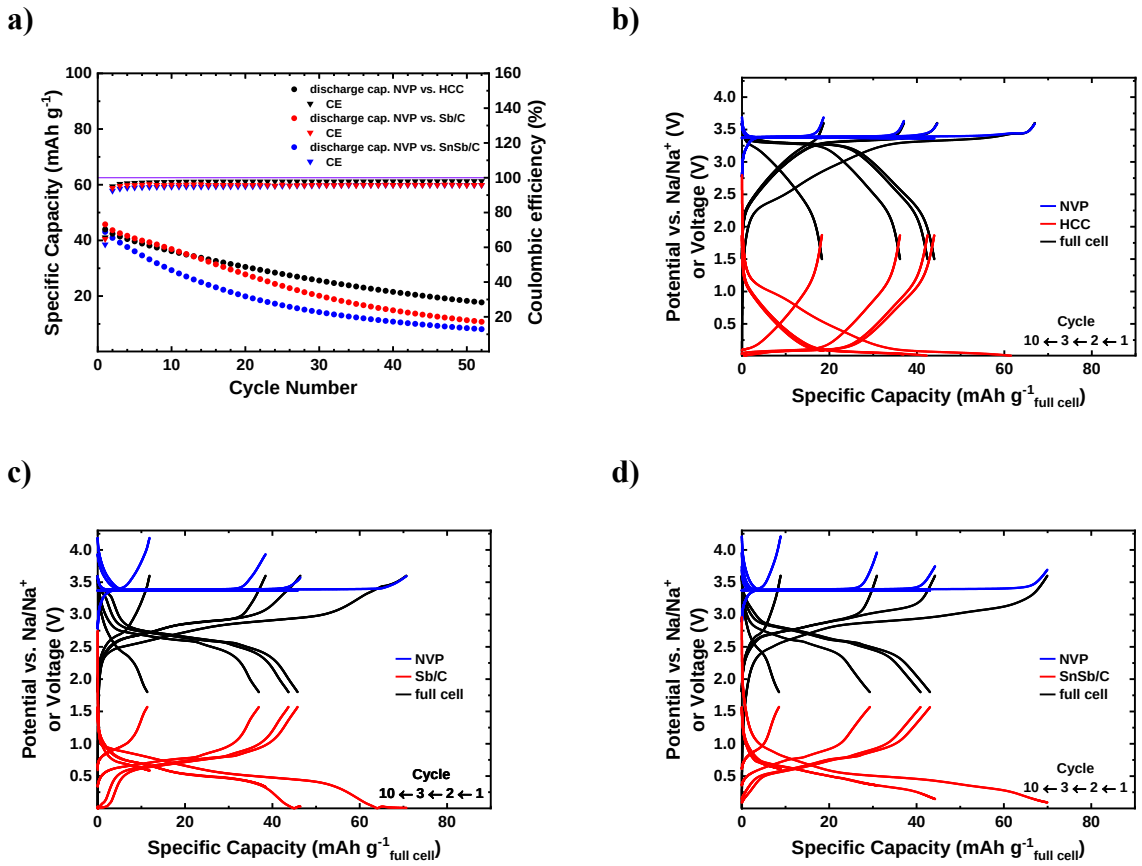

Figure 2. Electrochemical data of NVP/C cycled against HCC, Sb/C and SnSb/C (1 M $NaClO_4$ in EC/DMC (1:1) with 5 wt% FEC) in a three-electrode configuration with a specific current of 100 mA/g_{anode}. (a) Specific capacities and Coulombic efficiency of the NVP/C-HCC, NVP/C-Sb/C and NVP/C-SnSb/C cell; (b) full cell voltages and electrode potentials vs. Na/Na^+ for NVP/C-HCC in the voltage range between 1.5 V – 3.6 V; (c) for NVP/C-Sb/C in the voltage range between 1.8 V – 3.6 V and (d) for NVP/C-SnSb/C in the voltage range between 1.8 V – 3.6 V.

3.3) NVP/C cycled against Na metal

NVP-Na metal cells were already introduced at the beginning of this report. Here, we focus on the issues that arise upon operating the cells over many cycles. FEC does not only affect the occurrence of the second plateau, but also changes the long-term cycling behaviour. Fig. 1e shows the polarizations (potential of metal electrode vs. RE) of the metal anodes. The polarization depending

on the state of charge is shown and discussed in the supplements (Fig. S1a, b). In the NVP-Na metal setup with an FEC-containing electrolyte, the polarization of the counter electrode is relatively high during the first few cycles. It has been suggested that FEC leads to a multilayer SEI on the Na metal, which prevents reactions between the electrolyte and the Na metal [21, 33, 35]. The disadvantage of FEC is the strong polarization that we observe. The polarization slowly decreases over time (Fig. 1e). In contrast to that, without FEC the polarization of Na metal anode is negligible at the beginning, but it increases steadily during cycling due to increasing side reactions (Fig. 1e) [34].

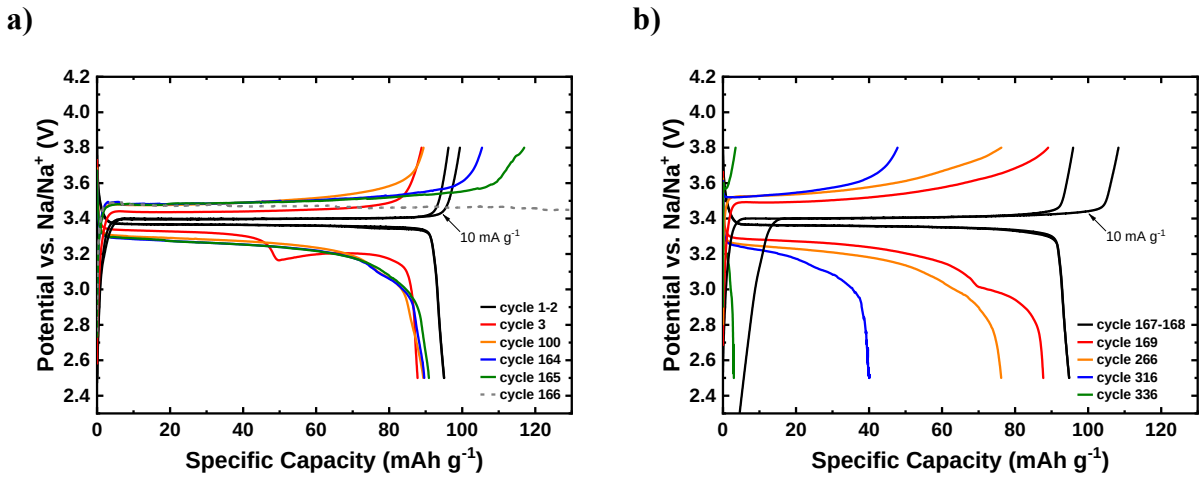

Figure 3. Electrochemical data of NVP/C cycled against sodium metal (1 M $NaClO_4$ in EC/DMC (1:1) with 10 wt% FEC) in a two-electrode configuration. (a) GCPL curves of NVP/C in the potential range between 2.5 V – 3.8 V vs. Na/Na^+ before and (b) after anode replacement with a specific current of 10 mA/g and 100 mA/g.

In Fig. 3a, selected charge and discharge curves of the standard NVP-Na metal cell are shown. After the initial two cycles at a current rate of 10 mA/g, the following cycles at 100 mA/g display a marginally lower specific discharge capacity of 90 mAh/g. For the most part, the CE of the cell is above 99.8 %. After 165 cycles the electrochemical behaviour of the cell changes abruptly:

During the desodiation step of the NVP/C electrode, the potential cannot be elevated above the voltage plateau at 3.4 V. In Fig. 3a, around 30 mAh/g, the dashed grey desodiation curve deviates from the green curve. This suggests that the electrochemical reaction is not due to the desodiation of NVP/C, instead it may be due to a sodium metal dendrite with SEI touching the NVP/C cathode. The Swagelok-type cell was disassembled and the cycled NVP/C electrode was rinsed and used for a second time in a new cell. The same NVP/C positive electrode was successfully cycled again with a new separator, new electrolyte, and a new Na foil (Fig. 3b). A similar number of cycles can be achieved, but this time the capacity loss is more gradual (Fig. 3b), suggesting a consumption of the electrolyte. We confirmed that after the second and third failure, the electrolyte/anode can be replaced to obtain a working cell again. This clearly shows that the reliability of the cell is limited by the Na metal anode. Since NVP/C seems to be far more reliable, suitable anode materials are needed.

3.4) NVP/C cycled against NVP/C

NVP/C can be used as an anode due to the existence of a plateau around 1.6 V (Fig. 1c). Therefore, it is obvious to examine symmetric NVP cells.

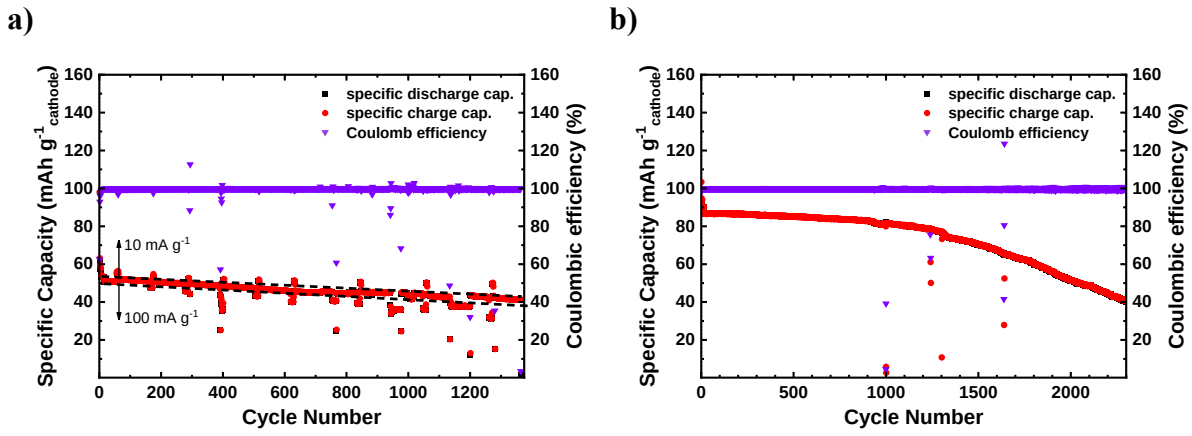

Figure 4. Electrochemical data of NVP/C cycled against NVP/C (1 M $NaClO_4$ in PC) in a two-electrode configuration. (a) Specific capacities and Coulombic efficiency in the voltage range

between 1 V – 3 V of the symmetric NVP/C-NVP/C cell (1:1 mass ratio) with a specific current of 10 mA/g, 50 mA/g or 100 mA/g and (b) of the balanced symmetric NVP/C-NVP/C cell (1:2 mass ratio) with a specific current of 10 mA/g or 100 mA/g.

In Fig. 4a, the GCPL results of the symmetric cell are shown for different specific currents in the voltage range between 1 V and 3 V. For this 1:1 mass ratio, only 60 mAh/g of the specific capacity of the NVP/C cathode are used and the capacities are unbalanced. Compared to the results presented so far, the reliability of the symmetric cell was very high, and we ended the experiment after more than 1300 cycles (Fig. 4a). Higher capacities can be achieved for a balanced cell of this type (Fig. 4b). Here, the NVP/C negative electrode contains twice the amount of the active material mass compared to the NVP/C positive electrode. While the CE is above 99.9 % and very stable over time, the initial specific capacity of 93 mAh/g steadily decreases to 40 mAh/g after 2300 cycles (Fig. 4b). In Fig. S3b, it is a shown that a better capacity retention may be possible. When NVP/C is cycled against sodium metal until the metal degrades (Fig. 3a,b), the NVP/C cathode is reusable in cells with an NVP/C anode and can be cycled again (Fig. S2a,b). In terms of cycling stability, the balanced NVP/C cells are far superior to all of the other cells reported in this work. This clearly shows that, when combined with a suitable anode, NVP/C used as cathode is highly reliable and that NVP/C as an anode material is stable over many cycles. Hence, NVP/C could serve as a benchmark and reference material for SIB, both as anode and cathode. As an anode, it exhibits low electrode polarization, high rate capability and has a well-defined voltage plateau around 1.6 V vs. Na/Na^+, where hardly any SEI will form. Compared to the alloy and metal anodes, the NVP exhibits a smaller volume change during cycling [36]. Besides the volume change, NVP/C is similar to lithium titanate $Li_4Ti_5O_{12}$ (LTO), which is a common reference electrode material for lithium-ion batteries (LIB). As a cathode, NVP/C is an electrode material with high

technological relevance for future sodium-based batteries with moderate energy density and high reliability.

4.) Conclusions

NVP/C composites were synthesized via the method of spray-drying and subsequent calcination. During galvanostatic cycling, NVP/C exhibits potential plateaus around 1.6 V and 3.4 V vs. Na/Na^+ and therefore can be used as anode or cathode material. We show that the use of sodium metal as anode can result in deceiving electrochemical data, in the form of deviations from the 3.4 V plateau. This is triggered by the use of FEC as an additive in the electrolyte. We combined NVP/C cathodes with anodes of Na metal, hard carbon, Sb/C and SnSb/C and obtained relatively poor capacity retention. On the contrary, using NVP/C both as anode and cathode, 1543 cycles were achieved with a capacity retention of 80 %. This demonstrates that NVP/C itself is a very reliable electrode material both as anode and as cathode. A large part of the limited cycling stability observed in this work and in the literature can be attributed to the anode material chosen. This is also important for electrochemical studies of other cathode materials. Fully symmetric NVP-NVP cells (1:1 mass ratio) are not recommended since they have reduced capacity and energy density compared to balanced cells (1:2 mass ratio). Our results are relevant for applications where the long-term stability is more important than high energy density: The balanced NVP-NVP cell is an example of a reliable sodium-ion cell. The NVP/C anode might be used to test and to compare the stability of sodium-ion cathode materials without the misleading degradation problems caused by the presence of metallic sodium or anode materials, which suffer from irreversible reactions. As a reference electrode for a three-electrode cell, a presodiated NVP/C is advantageous because of its stable potential, limited amount of SEI, and high capacity. The results for the balanced NVP-NVP cells demonstrate that NVP/C is a highly promising cathode material. Once a stable anode with

lower potential is available, this cathode material might be used to develop highly reliable and technologically relevant Na-based batteries.

Supporting Information: Additional experimental results and discussion

Corresponding Author

*Institute for Applied Materials (IAM), Karlsruhe Institute of Technology (KIT), Hermann-von-Helmholtz-Platz 1, 76344 Eggenstein-Leopoldshafen, Germany; E-mail: dominik.kramer@kit.edu

Author Contributions

The manuscript was written through contributions of all authors. All authors have given approval to the final version of the manuscript.

Acknowledgments

This work was funded by the Deutsche Forschungsgemeinschaft (DFG, German Research Foundation) under Germany´s Excellence Strategy – EXC 2154 – Project number 390874152. We thank Dr. Angelina Sarapulova for supporting scientific discussions.

References

1. Yang, Z., et al., *Electrochemical Energy Storage for Green Grid.* Chemical Reviews, 2011. 111(5): p. 3577-3613.

2. Ellis, B.L. and L.F. Nazar, *Sodium and sodium-ion energy storage batteries.* Current Opinion in Solid State and Materials Science, 2012. 16(4): p. 168-177.

3. Zatovsky, I.V., *NASICON-type $Na_3V_2(PO_4)_3$.* Acta Crystallographica Section E: Structure Reports Online, 2010. 66(2): p. i12-i12.

4. Song, W., et al., *A study into the extracted ion number for NASICON structured $Na_3V_2(PO_4)_3$ in sodium-ion batteries.* Physical Chemistry Chemical Physics, 2014. 16(33): p. 17681-17687.

5. Song, W., et al., *First exploration of Na-ion migration pathways in the NASICON structure $Na_3V_2(PO_4)_3$.* Journal of Materials Chemistry A, 2014. 2(15): p. 5358-5362.

6. Saravanan, K., et al., *The First Report on Excellent Cycling Stability and Superior Rate Capability of $Na_3V_2(PO_4)_3$ for Sodium Ion Batteries.* Advanced Energy Materials, 2013. 3(4): p. 444-450.

7. Duan, W., et al., *$Na_3V_2(PO_4)_3$@C core–shell nanocomposites for rechargeable sodium-ion batteries.* Journal of Materials Chemistry A, 2014. 2(23): p. 8668-8675.

8. Ling, R., et al., *Three-dimensional hierarchical porous $Na_3V_2(PO_4)_3$/C structure with high rate capability and cycling stability for sodium-ion batteries.* Chemical Engineering Journal, 2018. 353: p. 264-272.

9. Jian, Z., et al., *Carbon coated $Na_3V_2(PO_4)_3$ as novel electrode material for sodium ion batteries.* Electrochemistry Communications, 2012. 14(1): p. 86-89.

10. Jian, Z., Y. Sun, and X. Ji, *A new low-voltage plateau of $Na_3V_2(PO_4)_3$ as an anode for Na-ion batteries.* Chemical Communications, 2015. 51(29): p. 6381-6383.

11. Wang, D., et al., *$Na_3V_2(PO_4)_3$/C composite as the intercalation-type anode material for sodium-ion batteries with superior rate capability and long-cycle life.* Journal of Materials Chemistry A, 2015. 3(16): p. 8636-8642.

12. Fang, Y., et al., *Hierarchical carbon framework wrapped $Na_3V_2(PO_4)_3$ as a superior high-rate and extended lifespan cathode for sodium-ion batteries.* Advanced materials, 2015. 27(39): p. 5895-5900.

13. Plashnitsa, L.S., et al., *Performance of NASICON symmetric cell with ionic liquid electrolyte.* Journal of the Electrochemical Society, 2010. 157(4): p. A536.

14. Zhang, Y., H. Zhao, and Y. Du, *Symmetric full cells assembled by using self-supporting $Na_3V_2(PO_4)_3$ bipolar electrodes for superior sodium energy storage.* Journal of Materials Chemistry A, 2016. 4(19): p. 7155-7159.

15. Wang, W., et al., *A flexible symmetric sodium full cell constructed using the bipolar material $Na_3V_2(PO_4)_3$.* Journal of Materials Chemistry A, 2017. 5(18): p. 8440-8450.

16. Didwal, P.N., et al., *Synthesis of 3-dimensional interconnected porous $Na_3V_2(PO_4)_3$@C composite as a high-performance dual electrode for Na-ion batteries.* Journal of Power Sources, 2019. 413: p. 1-10.

17. Sadan, M.K., et al., *High power $Na_3V_2(PO_4)_3$ symmetric full cell for sodium-ion batteries.* Nanoscale Advances, 2020. 2(11): p. 5166-5170.

18. Noguchi, Y., et al., *Fabrication and performances of all solid-state symmetric sodium battery based on NASICON-related compounds.* Electrochimica Acta, 2013. 101: p. 59-65.

19. Bag, S., et al., *Electrochemical studies on symmetric solid-state Na-ion full cell using $Na_3V_2(PO_4)_3$ electrodes and polymer composite electrolyte.* Journal of Power Sources, 2020. 454: p. 227954.

20. Weingarth, D., et al., *Graphitization as a Universal Tool to Tailor the Potential-Dependent Capacitance of Carbon Supercapacitors.* Advanced Energy Materials, 2014. 4(13): p. 1400316.

21. Pfeifer, K., et al., *Interaction between Electrolytes and Sb_2O_3-Based Electrodes in Sodium Batteries: Uncovering the Detrimental Effects of Diglyme.* ChemElectroChem, 2020. 7(16): p. 3487-3495.

22. Manohar, C.V., et al., *Stability enhancing ionic liquid hybrid electrolyte for NVP@C cathode based sodium batteries.* Sustainable Energy & Fuels, 2018. 2(3): p. 566-576.

23. Mao, J., et al., *Scalable synthesis of $Na_3V_2(PO_4)_3$/C porous hollow spheres as a cathode for Na-ion batteries.* Journal of Materials Chemistry A, 2015. 3(19): p. 10378-10385.

24. Zhu, X., et al., *$Na_3V_2(PO_4)_3$/C nanocomposite synthesized via pre-reduction process as high-performance cathode material for sodium-ion batteries.* Journal of Alloys and Compounds, 2015. 646: p. 170-174.

25. Jiang, X., et al., *Extending the cycle life of $Na_3V_2(PO_4)_3$ cathodes in sodium-ion batteries through interdigitated carbon scaffolding.* Journal of Materials Chemistry A, 2016. 4(38): p. 14669-14674.

26. Guo, J.Z., et al., *A superior $Na_3V_2(PO_4)_3$-based nanocomposite enhanced by both N-doped coating carbon and graphene as the cathode for sodium-ion batteries.* Chemistry–A European Journal, 2015. 21(48): p. 17371-17378.

27. Chen, L., et al., *Hard Carbon Wrapped $Na_3V_2(PO_4)_3$@C Porous Composite Extending Cycling Lifespan for Sodium-Ion Batteries.* ACS Applied Materials & Interfaces, 2017. 9(51): p. 44485-44493.

28. Jiang, X., T. Zhang, and J.Y. Lee, *A Polymer-Infused Solid-State Synthesis of a Long Cycle-Life $Na_3V_2(PO_4)_3$/C Composite.* ACS Sustainable Chemistry & Engineering, 2017. 5(9): p. 8447-8455.

29. Li, X., et al., *High valence Mo-doped $Na_3V_2(PO_4)_3$/C as a high rate and stable cycle-life cathode for sodium battery.* Journal of Materials Chemistry A, 2018. 6(4): p. 1390-1396.

30. Wei, C., et al., *Voltage window-dependent electrochemical performance and reaction mechanisms of $Na_3V_2(PO_4)_3$ cathode for high-capacity sodium ion batteries.* Ionics, 2019: p. 1-9.

31. Chen, K.-H., et al., *Dead lithium: mass transport effects on voltage, capacity, and failure of lithium metal anodes.* Journal of Materials Chemistry A, 2017. 5(23): p. 11671-11681.

32. Mandl, M., et al., *Sodium metal anodes: Deposition and dissolution behaviour and SEI formation.* Electrochimica Acta, 2020. 354: p. 136698.

33. Pfeifer, K., et al., *Choosing the right carbon additive is of vital importance for high-performance Sb-based Na-ion batteries.* Journal of Materials Chemistry A, 2020. 8(12): p. 6092-6104.

34. Pfeifer, K., et al., *Can metallic sodium electrodes affect the electrochemistry of sodium-ion batteries? Reactivity issues and perspectives.* ChemSusChem, 2019. 12(14): p. 3312.

35. Han, B., et al., *Probing the Na metal solid electrolyte interphase via cryo-transmission electron microscopy.* Nature Communications, 2021. 12(1): p. 1-8.

36. Chen, S., et al., *Challenges and Perspectives for NASICON-Type Electrode Materials for Advanced Sodium-Ion Batteries.* Advanced Materials, 2017. 29(48): p. 1700431.

SUPPORTING INFORMATION

$Na_3V_2(PO_4)_3$ - a highly promising anode and cathode material for sodium-ion batteries

*Tolga Akçay [a], Marcel Häringer [a], Kristina Pfeifer [a], Jens Anhalt [a], Joachim R. Binder [a], Sonia Dsoke [a,b], Dominik Kramer *[a], and Reiner Mönig [a]*

[a] Institute for Applied Materials (IAM), Karlsruhe Institute of Technology (KIT), Hermann-von-Helmholtz-Platz 1, 76344 Eggenstein-Leopoldshafen, Germany

[b] Helmholtz-Institute Ulm for Electrochemical Energy Storage (HIU), P.O. Box 3640, 76021 Karlsruhe, Germany

Corresponding Author

*Institute for Applied Materials (IAM), Karlsruhe Institute of Technology (KIT), Hermann-von-Helmholtz-Platz 1, 76344 Eggenstein-Leopoldshafen, Germany; E-mail: dominik.kramer@kit.edu

The polarization during individual cycles are depicted in Fig. S1a, b. Without FEC, the polarization of the counter electrode in the third cycle is remarkably low. A notably higher polarization in the FEC-containing electrolyte happens during the NVP/C sodiation step. At a specific capacity of 61 mAh/g, when the maximum slope of the polarization curve is reached, the second plateau initiates (dotted line). Shortly after, a polarization peak of 0.091 V is reached, which corresponds to the value of the voltage drop between both plateaus in Fig. 1d. After 160 cycles, this peak is not present anymore and the slopes during sodiation and desodiation are very similar in shape. This is not the case for the NVP-Na metal cell without FEC, which demonstrates a large peak of 0.237 V in the polarization. While a second plateau might be expected, the overall behaviour is noticeably different. Here, much higher overpotentials are attained, which compensate for the lack of the second plateau in the GCPL measurement. Overall, this leads to faster degradation and ultimately to cell failure.

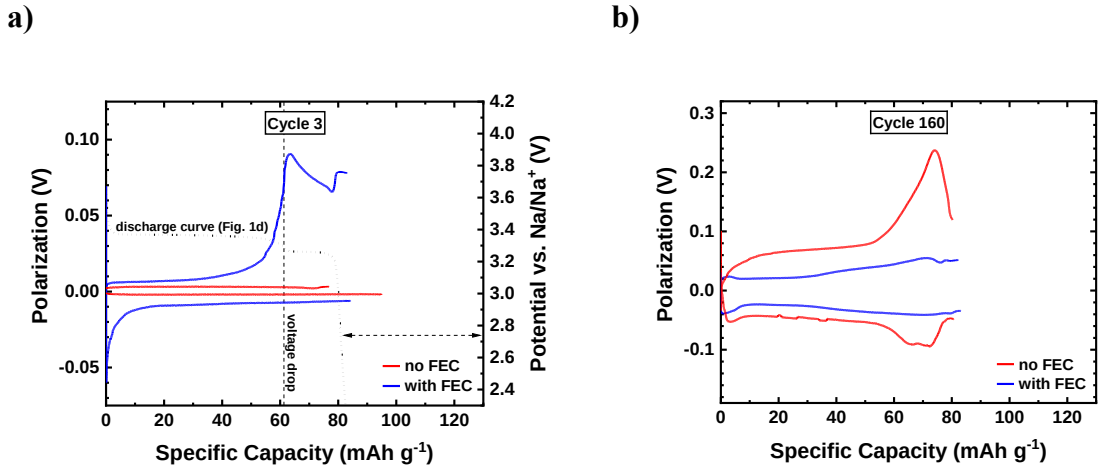

Figure S1. Electrochemical data of NVP/C cycled against sodium metal (1 M $NaClO_4$ in EC/DMC (1:1) without FEC or with 5 wt% FEC) in a three-electrode configuration with a specific current of 18 mA/g. (a) Polarization curves (potential of metal counter electrode vs. sodium RE) over specific capacity of the 3rd cycle and (b) of the 160th cycle during charge and discharge.

Without FEC as an additive, the specific capacity of NVP/C cycled in a new cell against sodium metal in a two-electrode configuration drops rapidly after 90 cycles at a specific current of 100 mA/g (Fig. S2a), which is 55 % of the 165 cycles that can be achieved by adding FEC to the electrolyte (Fig. 3a). The CE averages at 99 % in the first 90 cycles of Fig. S2a and is remarkably lower than the balanced cell in Fig. 4b. The cycled NVP/C cathode from Fig. S2a was mounted in a new cell with a balanced NVP/C anode. In this new cell, an increased average CE of 99.6 % and a highly stable specific capacity of 82 mAh/g were obtained (Fig. S2a, b). In contrast to the results from Fig. 3a and 3b, where fast degradation was observed after the exchange of the metal anode, without any Na metal the NVP/C cathode is stable for more than 200 cycles (Fig. S2b). Once more, this indicates that the anode failed in Fig. S2a, whereas the NVP/C used as cathode does not degrade.

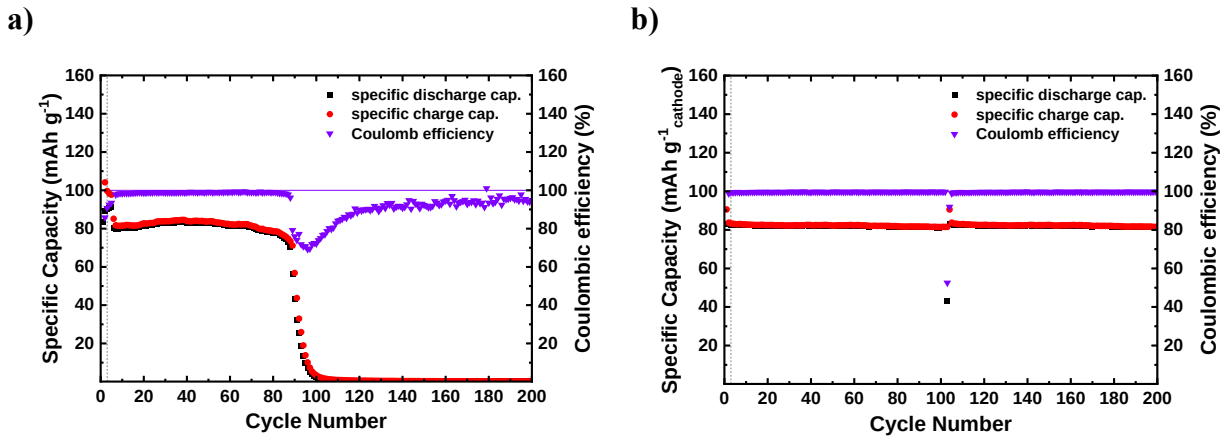

Figure S2. Electrochemical data of NVP/C cycled against sodium metal and then against a balanced NVP/C (1:2 mass ratio) anode (1 M $NaClO_4$ in EC/DMC (1:1)) in a two-electrode configuration. (a) Specific capacities and Coulombic efficiency of NVP/C cycled against sodium metal in the potential range between 2.5 V – 3.8 V vs. Na/Na^+ with a specific current of 10 mA/g or 100 mA/g and (b) of the balanced symmetric NVP-NVP cell in the voltage range between 1 V

– 3 V with a specific current of 10 mA/g or 100 mA/g after replacing the Na anode with a balanced NVP/C anode.

Fig. S3a shows the GCPL curves of the balanced NVP-NVP cell in a two-electrode configuration. During cycling the overpotential of the cell increases. At higher cycle numbers, this overpotential leads to limited sodiation, because the selected voltage limit is hit (blue curve). It can be assumed that with a lower cut-off voltage, less capacity fading will be observed. As can be seen in Fig. 4b or S3b, the capacity decreases with different slopes depending on the cycle number. Starting around 1200 cycles, degradation becomes faster, which may be caused by incomplete sodiation due to the chosen potential limit. An extrapolation using the initial slop is shown in Fig. S3b. This would lead to nearly 3200 cycles for a capacity retention of 80 %.

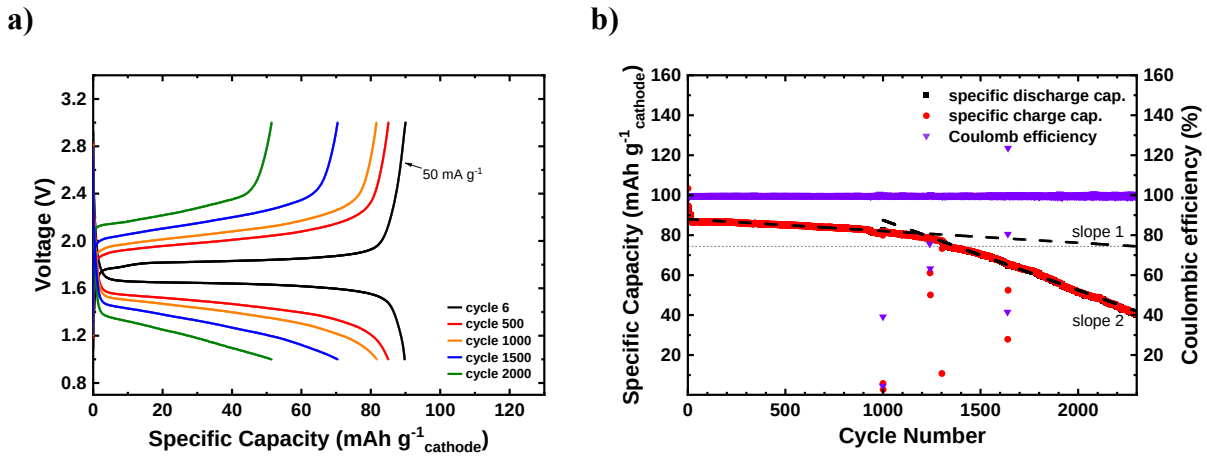

Figure S3. Electrochemical data of NVP/C cycled against NVP/C (1 M $NaClO_4$ in PC) in a two-electrode configuration. (a) GCPL curves of the balanced symmetric NVP/C-NVP/C cell in the voltage range between 1 V – 3 V with a specific current of 50 mA/g or 100 mA/g and (b) specific capacities and Coulombic efficiency of the balanced symmetric NVP/C-NVP/C cell in the voltage range between 1 V – 3 V with a specific current of 10 mA/g or 100 mA/g.